IEEE Access
Multidisciplinary | Rapid Review | Open Access Journal

Received November 8, 2018, accepted November 28, 2018, date of publication December 4, 2018,
date of current version December 31, 2018.

Digital Object Identifier 10.1109/ACCESS.2018.2884947

Model-Data Driven Learning Adaptive Robust Control of Precision Mechatronic Motion Systems With Comparative Experiments

CHUXIONG HU[1,2], (Senior Member, IEEE), ZHIPENG HU[1,2], YU ZHU[1,2], (Member, IEEE), ZE WANG[1,2], AND SUQIN HE[1,2]

[1]State Key Laboratory of Tribology, Department of Mechanical Engineering, Tsinghua University, Beijing 100084, China
[2]Beijing Key Laboratory of Precision/Ultra-Precision Manufacturing Equipments and Control, Tsinghua University, Beijing 100084, China

Corresponding author: Chuxiong Hu (cxhu@tsinghua.edu.cn)

This work was supported in part by the National Nature Science Foundation of China under Grants 51775305 and 51475262, in part by the Autonomous Scientific Research Project of Tsinghua University under Grant 20151080363, and in part by the Autonomous Research Project of the State Key Laboratory of Tribology, Tsinghua University, under Grant SKLT2018C02.

ABSTRACT In order to meet the rigorous motion accuracy requirement and efficiently utilize the repetitive-task characteristics in modern precision industry, this paper concentrates on the comprehensive research of model-based data-driven learning adaptive robust control (LARC) strategy for precision mechatronic motion systems. The proposed LARC can achieve not only excellent transient/steady-state tracking performance but also adaptation ability and disturbance robustness. Specifically, the LARC strategy contains robust feedback term, adaptive model compensation term, and iterative learning term. Herein, the former two terms are designed based on the system dynamic model under parametric uncertainty and uncertain nonlinearity, and the data-driven iterative learning term is synthesized to generate optimal input to adjust the optimal reference. The whole controller design procedure and stability is presented, while the reason for the practically achievable performance of LARC is analyzed. Comparative experiments, among proportional—integral—differential, adaptive robust control, iterative learning control, and the proposed LARC, are conducted on a developed linear motor stage. The experimental results consistently validate that the proposed LARC scheme simultaneously achieves excellent transient/steady-state tracking performance, parametric adaptation ability, and disturbance robustness. The LARC strategy essentially provides an effective control technology with good potential in industrial applications.

INDEX TERMS LARC, motion control, linear motor, tracking accuracy, adaptive control, iterative learning.

I. INTRODUCTION

Modern precision/ultra-precision mechatronic equipments such as lithography wafer/reticle stages, machine tools, laser cutting machines, and robotic manipulators, require intelligent motion control technologies [1]–[5]. When the motion control accuracy requirements are macro/nano-meter level, the effects of model uncertainty and uncertain disturbance cannot be neglected, and even become the major obstacle to achieving excellent transient/steady-state tracking performance. This problem has been extensively studied and many advanced control methods are resultantly developed [6]–[10]. A typical scheme is adaptive robust control (ARC) which possesses good parametric adaptive capability and robustness to nonlinear uncertainties/disturbances [11]–[13]. Subsequent ARC studies have been applied to theory extension and practical mechatronic applications such as linear motor driven systems, pneumatic muscles, and hydraulic manipulators [14]–[19]. However, ARC primarily depends on the plant system model and has certain conservativeness on practical steady-state tracking accuracy.

In modern industry, mechatronic systems often have complex structures and uncertainties those make it difficult to obtain accurate motion control models. Meanwhile, industry systems often perform repetitive motion tasks in a limited time. Therefore, iterative learning control (ILC) scheme is constructed as a feedforward control scheme based on repetitive task over a finite time horizon [20]. ILC utilize the information from previous iteration data to generate optimal control input. The advantage of ILC is that, it can achieve good control performance without need of accurate

dynamics model, which is very important for mechatronic motion control systems with significant nonlinearity and complexity [21]. For nearly two decades, ILC has been extended and applied to wafer stages and robots [22]–[24]. The basic idea of ILC is easy for practical engineer to understand, yet sustained effort is needed to analyze appropriate structure and update rule to handle robustness and optimization issues [25]. However, ILC needs several iteration learning experiments to generate the final optimal control input, while is rather sensitive to non-repetitive disturbance and noise, which leads to application limitations in industry [26]. For example, if there exist distinct load variation or random disturbance, the tracking accuracy of the data-driven ILC will deteriorate significantly [27].

It can be summarized that, ARC guarantees transient performance with parameter adaptation capability and disturbance robustness, while the steady-state tracking performance is conservative due to the existence of unmodelled dynamics. On the other hand, ILC does not need accurate system model and has excellent steady-state tracking accuracy, but with issues of sensitivity to non-repetitive disturbance and parametric uncertainty. In current researches, newly developed advanced control methods such as neural networks [28] and repetitive control [29] combined with ARC further improve transient and steady-state tracking performance. However, the resulting controllers are theoretically complicated, and the steady-state tracking performances still have performance improvement potential [30], [31]. On the other hand, considering the characteristics of ILC, researchers are also trying to explore other advanced control methods to fill the disadvantages of ILC to improve control scheme [25]. As an illustration, research has been undertaken to study iteration learning schemes in adaptive control using Lyapunov like methods [32]. However, due to different research backgrounds, rigorous theoretical deduction and analysis are of main concern in the above researches, while the application to precision industry systems is reported limitedly.

In this paper, inspired by the idea that the advantages and disadvantages of ARC and ILC can be mutually complementary, and the fact that the practical plant system model cannot be completely accurate for perfect model compensation, we completely present a model-based data-driven learning adaptive robust (LARC) controller for mechatronic systems to practically achieve high performance. This research can also be considered as significant theory and application extension of our previous preliminary attempt in [33]. Specifically, the LARC framework scheme includes iterative learning term, adaptive compensation term, and robust feedback term. The first term is designed to create optimal input to adjust the optimal reference, while the later two terms are designed based on the system dynamics model under parametric uncertainty and uncertain nonlinearity. The whole controller design procedure and stability is presented, while the reason for the practically achievable performance of LARC is analyzed. Comparative experiments among PID, ARC, ILC, and the proposed LARC, are conducted on a developed linear motor stage under different tracking motions. The experimental results consistently validate that the proposed LARC scheme performs much better than the other controllers while the practical performances can meet the challenge of external disturbances and load variation. In other word, the proposed scheme simultaneously achieves excellent transient/steady-state tracking performance, parametric adaptation ability, and disturbance robustness. The proposed LARC essential offers an effective motion control technology for industrial implementation, and also supplies another perspective for control engineers.

II. MODEL-BASED DATA-DRIVEN LEARNING ADAPTIVE ROBUST CONTROL (LARC) STRATEGY

In order to facilitate understanding of the LARC control scheme, consider a second-order electromechanical device system (e.g., the linear motor driven stage system) which is common in practical industry, i.e.,

$$\theta_1 \ddot{x} = \varphi(\dot{x}, x, t)^T \vartheta + \Delta(x, t) + u \tag{1}$$

where x means the position of the motion stage, u represents the control input, θ_1 is the unknown parameter of the system, ϑ is an unknown parameter matrix, $\varphi(\dot{x}, x, t)$ is a known shape function set, and $\Delta(x, t)$ means the set of all the uncertainties. According to the definition of $\theta = [\theta_1, \vartheta]^T$, we can obtain the following assumption, i.e., the ranges of uncertainties of parameters and disturbances are limited by

$$\begin{aligned} \theta \in \Omega_\theta &\triangleq \{\theta : \theta_{min} < \theta < \theta_{max}\} \\ \Delta \in \Omega_\Delta &\triangleq \{\Delta : \|\Delta(x, t)\| \leq \delta\} \end{aligned} \tag{2}$$

where θ_{min}, θ_{max} and δ are known.

In order to track the desired trajectory $x_d(t)$, i.e., $x(t) \to x_d(t)$, the schematic of LARC control scheme with the serial structure is plotted in Fig. 1. It is well shown in Fig. 1 that, the green part means the iterative learning control (ILC) term, the function of the brown part is adaptive compensation, the blue part is responsible for robust feedback control, and the yellow one is the plant. Herein, the adaptive compensation and robust feedback control constitute of the ARC term which is the purple part. As illustrated in Fig. 1, ILC, i.e., the green part, can be viewed as a kind of trajectory optimization which can achieve excellent compensation of unmodelled repetitive uncertainty using the repetitive historical control data such as tracking error $e = x - x_d$. Through the additional input u_{ILC} generated by ILC, the desired trajectory x_d can be adjusted to $x_d' = x_d + u_{ILC}$ which is essentially a new trajectory to be followed by the ARC control term. And then, parameter adaptation, model compensation and robust feedback control are synthesized in ARC term based on the plant model and the adjusted tracking error $e' = x - (x_d + u_{ILC}) = x - x_d'$. It is easy to find in the schematic that the ILC and the ARC term belongs to feedforward and feedback control, respectively. Herein, the stability of whole control system just depends on the closed-loop characteristics of ARC and the plant. Essentially, the optimal trajectory pre-compensation

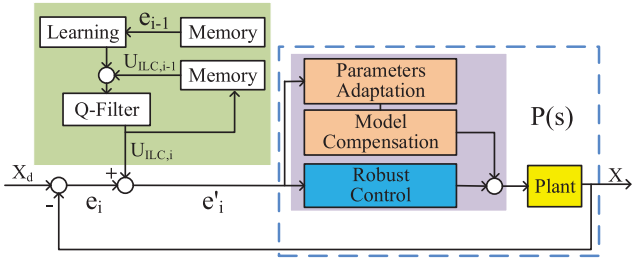

FIGURE 1. LARC control strategy in a serial structure.

should be obtained through the ILC term which can improve tracking performance significantly in practical applications. It should be noted that, the serial structure employed here facilitates the theory conduction and practical implementation, when compared to others such as the parallel structure shown in [34]. In the following, the different terms the proposed LARC scheme, i.e., ARC and ILC will be introduced, respectively.

A. ADAPTIVE ROBUST CONTROL (ARC) TERM IN LARC

Basically, ARC combines the advantages of conventional adaptive control and deterministic robust control, and has good adaptability to parameter changes and robustness to uncertain disturbances [11]. With the schematic of LARC framework shown in Fig. 1, the ARC term is designed with adjusted model compensation and robust feedback as follows.

Firstly, a switching-function quantity is defined as

$$p = \dot{e}' + k_1 e' = \dot{x} - x_{eq}, \quad x_{eq} \triangleq \dot{x}'_d - k_1 e' \tag{3}$$

where k_1 is any positive feedback gain; $e' = x-(x_d+u_{ILC}) = x - x'_d$ is the adjusted tracking error while $e = x - x_d$ is the actual tracking error. Differentiate (3) and notice (1):

$$\begin{aligned} \theta_1 \dot{p} &= \varphi(\dot{x}, x, t)^T \vartheta - \theta_1 \dot{x}_{eq} + \Delta(x,t) + u \\ &= \phi(\dot{x}, x, t)^T \theta + \Delta(x,t) + u \end{aligned} \tag{4}$$

where $\phi(\dot{x}, x, t)^T = [-\dot{x}_{eq}, \varphi(\dot{x}, x, t)^T]$ and $\theta = [\theta_1, \vartheta]^T$. Noting the structure of Eq. (4), we can design the ARC control term as [13]

$$\begin{aligned} u &= u_f + u_s, \quad u_f = -\phi(\dot{x}, x, t)^T \hat{\theta} \\ u_s &= u_{s1} + u_{s2}, \quad u_{s1} = -k_s p \end{aligned} \tag{5}$$

where u_f is the model compensation required for perfect trajectory tracking, $\hat{\theta}$ is the estimated parameter, u_s represents the feedback control term, u_{s1} is a simple proportional feedback item, and u_{s2} is a robust feedback term which is detailedly explained in [11] and [31].

The estimated parameter $\hat{\theta}$ in the ARC term is updated by the following parameter adaptive rules which is a kind of discontinuous projection.

$$\dot{\hat{\theta}} = Proj_{\hat{\theta}}(\Gamma\tau),$$
$$Proj_{\hat{\theta}}(\bullet_i) = \begin{cases} 0, & if\ \hat{\theta}_i = \theta_{imax}\ and\ \bullet_i > 0 \\ 0, & if\ \hat{\theta}_i = \theta_{imin}\ and\ \bullet_i < 0 \\ \bullet_i, & otherwise \end{cases} \tag{6}$$

where τ is an adaptation function; Γ is any diagonal symmetric positive definite adaptation rate matrix. Define the projection map $proj_{\hat{\theta}}(\cdot)$ to ensure that the boundary of parameter is the same as Eq. (2).

As shown in [11], for any adaption function τ, the projection mapping expressed in (6) satisfies the following conditions:

$$\begin{aligned} &\mathbf{E1} \quad \hat{\theta} \in \Omega_\theta \triangleq \{\hat{\theta} : \theta_{min} \le \hat{\theta} \le \theta_{max}\} \\ &\mathbf{E2} \quad \tilde{\theta}^T(\Gamma^{-1} Proj_{\hat{\theta}}(\Gamma\tau) - \tau) \le 0, \quad \forall\tau \end{aligned} \tag{7}$$

Substitute Eq. (5) into (4), and then simplify the resulting expression:

$$\theta_1 \dot{p} = u_s - \phi(\dot{x}, x, t)^T \tilde{\theta} + \Delta(x,t) \tag{8}$$

where $\tilde{\theta}$ is the estimation deviation (i.e., $\tilde{\theta} = \hat{\theta} - \theta$). Noting (2) and **E1** of (7), there exists a u_{s2} so the following two conditions are satisfied, i.e.,

$$\begin{aligned} &\text{i} \quad p\{u_{s2} - \phi\tilde{\theta} + \Delta\} \le \varepsilon \\ &\text{ii} \quad p u_{s2} \le 0 \end{aligned} \tag{9}$$

where ε is a parameter designed to be arbitrarily small. Essentially, i of Eq. (9) shows that the model uncertainties from parametric uncertainties as well as uncertain nonlinearities are dominated by the synthesized u_{s2}.

And ii of (9) is to make sure that u_{s2} dissipates naturally so that it does not interfere with the function of the adaptive control term.

Theorem 1: If the adaptation function expressed in Eq. (6) is set to

$$\tau = \phi(x) p \tag{10}$$

Then for the closed-loop control system, the ARC control term (5) of the proposed LARC approach can achieve the following results:

1) Generally, all signals are bounded and the positive definite function V_s defined by $V_s = \frac{1}{2}\theta_1 p^2$, is bounded by

$$V_s \le \exp(-\lambda t) V_s(0) + \frac{\varepsilon}{\lambda}[1 - \exp(-\lambda t)] \tag{11}$$

where $\lambda = 2k_s/\theta_{1max}$.

2) If after a limited time t_0, there is only parametric uncertainty, then the tracking error converges to zero finally, i.e., $e' \to 0$ and $p \to 0$ as $t \to \infty$.

Proof: Noting (5) and (8), we can obtain

$$\dot{V}_s = -k_s p^2 + p\{u_{s2} - \phi\tilde{\theta} + \Delta\} \tag{12}$$

According to condition i of (9), and choosing $\lambda = min\{2k_s/\theta_{1max}\}$, we have

$$\dot{V}_s \le -k_s p^2 + \varepsilon \le -\lambda V_s + \varepsilon \tag{13}$$

the above inequation leads to (11) and proves the results in 1) of the Theorem 1. Now consider the situation in 2) of Theorem 1, i.e., $\Delta = 0, \forall t \ge t_0$. Choosing the function V_a as

$$V_a = V_s + \frac{1}{2}\tilde{\theta}^T \Gamma^{-1} \tilde{\theta} \tag{14}$$

From (12), condition ii of (9) and P2 in (7), the derivative of V_a satisfies

$$\dot{V}_a = \dot{V}_s + \tilde{\theta}^T \Gamma^{-1} \dot{\tilde{\theta}} \leq -k_s p^2 + \tilde{\theta}^T \Gamma^{-1} (\dot{\tilde{\theta}} - \Gamma \tau) \leq -k_s p^2 \tag{15}$$

Therefore, $p \in L_2$. Intuitively, $\dot{p}$ is bounded. Accordingly, p is uniformly continuous. By Barbalat's lemma, $p \to 0$ as $t \to \infty$. ■

Remark 1: One smooth example of u_{s2} which satisfies (9) can be found in the following way [11]. Let h be any smooth function satisfying

$$h \geq \| \theta_M \| \| \phi \| + \delta \tag{16}$$

where $\theta_M = \theta_{max} - \theta_{min}$. Then, u_{s2} can be chosen as

$$u_{s2} = -\frac{1}{4\varepsilon} h^2 p \tag{17}$$

It should be noted that the asymptotically stability is satisfied under null disturbance assumption, which is unrealistic in practice. Therefore, the tracking error inevitably exists. Detailed analysis about this situation will be explained in next subsection. Through Theorem 1, the stability of the system is guaranteed as the feedforward ILC term in Fig. 1 does not affect the stability but just do a trajectory pre-compensation job. The ILC design would be described in the following section.

B. ITERATIVE LEARNING CONTROL (ILC) TERM IN LARC

ILC delivers outstanding stable tracking performance under repetitive tasks without the need for an accurate system model. Notice the serial LARC structure in Fig. 1, which iteratively learns to generate inputs to change the reference of ARC. If the closed-loop dynamics of ARC controller and the plant are expressed as $P(s)$ shown as the blue dashed line frame in Fig. 1, with the denotation of $P(s)$, the whole LARC control system can be described by

$$X_i(s) = P(s)[U_{ILC,i}(s) + X_d(s)] \tag{18}$$

where i means the iteration index. To obtain the optimal ILC input, an iteration learning law is used as

$$U_{ILC,i+1}(s) = Q(s)(U_{ILC,i}(s) + L(s)E_i(s)) \tag{19}$$

In Eq. (19), $U_{ILC,i+1}(s)$ is the input in $i+1$ iteration, $E_i(s)$ is the tracking error in i iteration, $L(s)$ represents learning function to generate ILC input used in the next iteration, and $Q(s)$ is the Q-filter which can limit learning bandwidth for robustness at the expense of tracking performance. As we all know, the design methods of learning function mainly include several types, namely PD-Type adjustable design, plant inversion, H_∞ method and quadratically optimal design [26]. PD-type tunable ILC learning function due to its simple structure and tunability for PD-type tunable designs:

$$L(s) = K_{ip} + K_{id} s \tag{20}$$

Accordingly, stability and convergence of the iterative learning rule defined in Eq. (19)-(20) can be guaranteed under certain conservative condition [26].

Lemma 1: The ILC law Eq. (19)-(20) acting on the stable system $P(s)$, is monotonically convergent, i.e., $\|E_\infty(s) - E_{i+1}(s)\|_\infty < \alpha \|E_\infty(s) - E_i(s)\|_\infty$ where α is the convergence rate, if

$$\|Q(s)(I - L(s)P(s))\|_\infty < \alpha < 1 \tag{21}$$

Substantially, Lemma 1 is to assurance that the output of ILC control $U_{ILC,i}$ converges to the optimal one which can capture the effects of the unmodeled repetitive uncertainties and achieve an effective compensation for the residual tracking errors. Consequently, once the ILC term is convergent as stated in Lemma 1, i.e., the U_{ILC} is optimally designed, it can be concluded that the stability of the whole control system is guaranteed.

As illustrated in Theorem 1, if there only is parametric uncertainty, zero final tracking error can also be achieved, which is theoretically equivalent to that $P(s)$ in Fig. 1 can be viewed as $P(s) = 1$. Then, substituting Eq. (20) into (21), the convergence condition can thus be obtained

$$\|Q(s)(I - K_{ip} - K_{id} s)\|_\infty < \alpha < 1 \tag{22}$$

Intuitively, Eq. (22) illustrate that, if $K_{ip} = 1$ and $K_{id} = 0$, the ideal convergence rate could be chosen as $\alpha = 0$, and the ILC term will achieve converged error after only one iteration. In Theory, the resultant feedforward signal u_{ILC} would be optimized by just one iteration. Simulation was conducted in our previous attempt [33] that the ILC term could significantly attenuate the low-frequency tracking error part and not amplify the high-frequency error part. It was also shown by simulation that $K_{ip} = 1$ is a good learning gain, which enabled guaranteed learning after one iteration. The effect of K_{id} is also examined with different values and the results showed that when $K_{id} \leq 1$, there are no distinct differences in learning performance, but when K_{id} is too large, the learning process will be unstable. Considering the analysis and simulation results in [33], learning gain $K_{ip} = 1$ and $K_{id} = 0$ will be used in experiments to provide an example. Researcher also could design more advanced ILC term as research extension of the proposed LARC scheme.

C. PRACTICAL NATURE OF LARC

In the proposed LARC algorithm, the ARC part is responsible to track $x'_d = x_d + u_{ILC}$ as accurately as possible. Actually, there is inevitable tracking error even the stability can be guaranteed theoretically as stated in Theorem 1. In other word, $e' = x - x'_d$ cannot be zero in practical applications, which means $e' = \zeta$ is consequent where ζ is the residual tracking error of the practical motion system. Noting $e' = e + u_{ILC}$, one obtains

$$e + u_{ILC} = \zeta \tag{23}$$

Consequently, if the characteristics of the residual error ζ could be captured by the optimal ILC feedforward signal

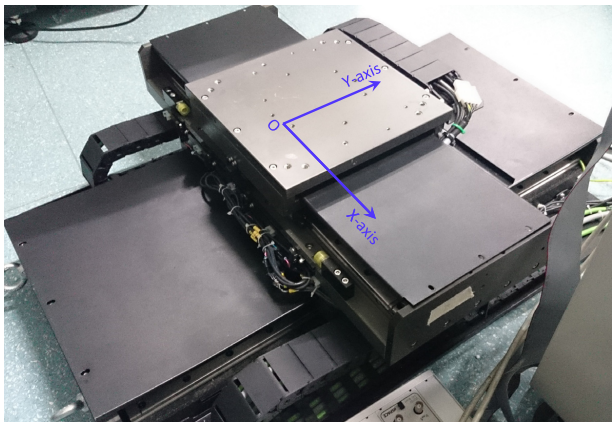

FIGURE 2. Experimental setup.

u_{ILC} as accurately as possible, i.e., $u_{ILC} \to \zeta$, a really ideal performance of the real tracking error e could achieve, i.e., $e \to 0$. This is the key essence of the proposed LARC control framework which makes sense of excellent tracking performance in practical applications. In the LARC control scheme, the ILC term is chosen as a typical one which may be simple to some degree. More advanced ILC based term [26] can also be extended under the proposed control framework.

III. COMPARATIVE EXPERIMENTAL STUDIES

A. EXPERIMENTAL SETUP

In this paper, the proposed LARC method is tested on an industrial linear motor shown in Fig. 2. The mechanical resonant modes and electrical dynamics are neglected in the linear motor system model, and the mathematical model is listed as follows [12], [13]:

$$M\ddot{x} = u - F, \quad F = F_f + F_r + F_d \tag{24}$$

where x means the position of the motor, M is the mass of the inertia load, u is the control input, F is the normalized lumped effect of the uncertain nonlinearities such as friction force F_f, ripple force F_r and external disturbance F_d. We choose to model the friction force as a function of velocity [35], [36], i.e., $F_f(\dot{x}) = B\dot{x} + A_f S_f(\dot{x})$. And the ripple force F_r is simply considered as part of the disturbance F_d. Therefore, Eq. (24) can be rewritten as

$$M\ddot{x} = u - B\dot{x} - A_f S_f(\dot{x}) - F_d \tag{25}$$

where A_f is the unknown static value of Coulomb friction term, B is an equivalent viscous friction coefficient, and $S_f(\dot{x})$ is a continuous function, e.g., $S_f(\dot{x}) = \frac{2}{\pi} arctan(2000\dot{x})$ which is an approximate expression for the Coulomb friction [12], [29], [35]. It can be seen that Eq. (25) is in the form of Eq. (1). The unknown parameter set is defined as $\theta = [\theta_1, \theta_2, \theta_3, \theta_4]^T$ where $\theta_1 = M$, $\theta_2 = B$, $\theta_3 = A_f$, $\theta_4 = F_d$, while $\phi(x) = [-\dot{x}_{eq}, -\dot{x}, -S_f(\dot{x}), -1]^T$ [13].

In the following, the controller described in Section II for the plant (25) would be tested on the linear motor stage. The position sensor for feedback is an optical grating scale with a resolution of 156.25 nm. System identification based on least-square is implemented to get the parameters of the X-axis of the linear motor driven stage. The approximate nominal values of θ_1, θ_2, θ_3 and θ_4 are: $\hat{\theta}_1 = 0.18Vs^2/m$, $\hat{\theta}_2 = 1.14Vs/m$, $\hat{\theta}_3 = 0.37V$, $\hat{\theta}_4 = 0$. The parameter variation bounds are determined based on the system identification results, i.e.,

$$\begin{aligned} \theta_{min} &= [0.15, 0.80, 0.20, -2.00] \\ \theta_{max} &= [0.30, 1.60, 1.50, 2.00] \end{aligned} \tag{26}$$

The control algorithms are tested on the linear motor through dSPACE DS 1106 controller system [35], [36]. The control algorithms are executed at a sampling frequency of $f_s = 5\ kHz$.

For fair comparison, several performance indexes will be employed to evaluate the practical quality of the control algorithms [35], i.e.,

- e_{RMS}: the root-mean-square (RMS) value of the tracking error.
- e_M: the maximal absolute value of the tracking error.

B. COMPARATIVE EXPERIMENTAL RESULTS

For sufficient comparison, four controllers, i.e., PID, ARC, ILC, and the proposed LARC controllers are all carried out as follows:

C1: PID — A parallel PID form is used with the expression like

$$C(s) = K_p + K_i/s + K_d s \tag{27}$$

Frequency identification of the linear motor motion stage system is conducted, and the open-loop frequency-domain characteristic is illustrated in Fig. 3. According to the frequency response shown in Fig. 3, the PID parameters are set as $K_p = 48000$, $K_i = 3200000$, $K_d = 100$. As a result, the open-loop crossover frequency is 135Hz, the phase-margin is 40.1deg, and gain-margin is 10.8dB. It should be noticed that these margins are all at a practically common level to ensure the system stability. Herein, considering actual situations to attenuate high frequency noise, the PID controller connects a first-order low-pass filter whose cutoff frequency is 3000Hz.

C2: ARC — The control scheme introduced in Section II-A while the ILC term is unused. Actually, there exist certain link between PID control parameters and ARC control parameters [13], i.e.,

$$\begin{cases} -K_p + \dfrac{K_i}{k_1} + K_d k_1 = 0 \\ \dfrac{K_i}{k_1} = \gamma_4 \\ K_d = k_s \end{cases} \tag{28}$$

Therefore, the control parameters of ARC are determined by the control parameters in C1 through Eq. (28) for a fair comparison. The resultant control parameters are $k_1 = 400$, $k_s = 100$, and $\gamma_4 = 8000$. In addition, the adaptation rate matrix is $\Gamma = diag[10, 10, 1, 8000]$, while the parameter initial estimates are chosen as $\hat{\theta}(0) = [0.15, 0.80, 0.20, 0]^{\mathrm{T}}$.

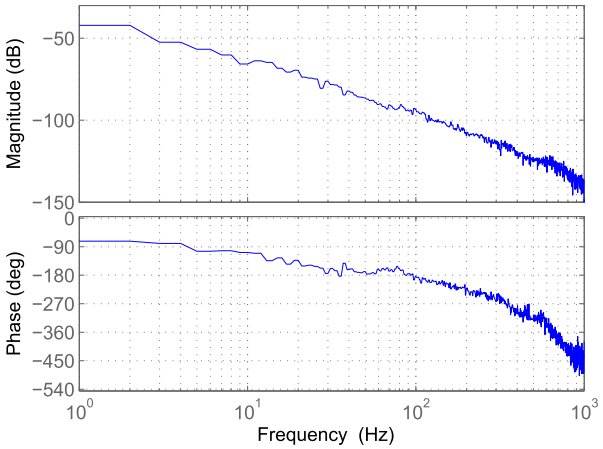

FIGURE 3. Frequency response of the linear motor.

C3: ILC — The controller introduced in Section II-B while the ARC term is unused. In this ILC controller, the feedback term is chosen as same as the above PID feedback control of C1. It is known in [23] that zero-phase filter can attenuate the bad transients and has application merit. In this paper, for no phase lag, the filter is designed as $F(s) = \frac{(2\pi f_s)^2}{s^2+2\zeta(2\pi f_s)+(2\pi f_s)^2}$ with damping ratio $\zeta = 0.7$ whose crossover frequency is $f_s = 80\ Hz$.

C4: LARC — The controller proposed in whole Section II. In LARC, the ARC term is the same as C2, and the iteration learning law is the same as C3. Moreover, all the controller and filter parameters of LARC here are set the same as those parameters in C2 & C3.

To further illustrate the tracking performance, the following three test sets are implemented:

- Set1: experiments without payload for testing the nominal tracking performance.
- Set2: a 12kg load is fixed on the motor mover to test the performance robustness to parameter uncertainty.
- Set3: 1.5V input is added to the control at 5.2s and removed at 7.2s to test the performance robustness to uncertain disturbance.

It must be pointed out that, in Set2 and Set3, the payload and the disturbance are all added in the case that the control inputs are determined in the nominal case (i.e., Set1), which is meaningful in industrial applications.

1) CASE I– HIGH SPEED SINUSOIDAL TRACKING MOTION

Firstly, the linear motor is to track a high speed sinusoidal trajectory like

$$x_d = 0.05 \cdot \sin(4\pi t - \pi/2) + 0.05(m) \tag{29}$$

with a speed of $v = 0.628\cos(4\pi t - \pi/2)m/s$ and an angular velocity of $\omega = 12.56\ rad/s$.

Table 1 shows the experimental results after running the linear motor stage for several periods. It should be noticed that, the control performance under point-to-point tracking motion in Case II and III will illustrate explicitly the transient

TABLE 1. Tracking performance indexes in Case I.

Controller		C1: PID	C2: ARC	C3: ILC	C4: LARC
Set1	$e_{RMS}(\mu m)$	6.50	3.32	3.44	2.52
	$e_M(\mu m)$	20.0	13.4	16.5	12.8
Set2	$e_{RMS}(\mu m)$	8.75	3.21	4.16	2.38
	$e_M(\mu m)$	21.7	12.1	20.8	11.5
Set3	$e_{RMS}(\mu m)$	6.61	3.70	3.89	2.85
	$e_M(\mu m)$	43.5	34.3	40.0	31.4

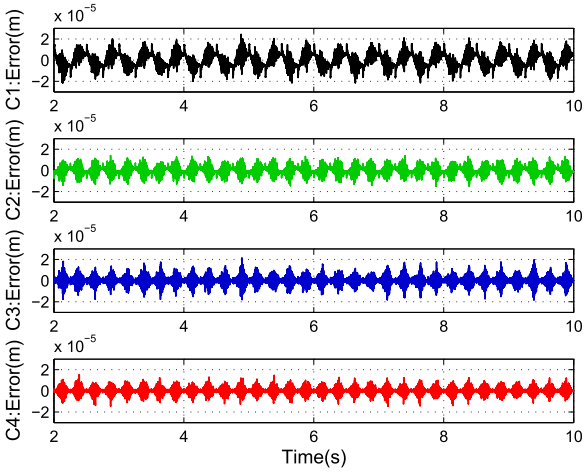

FIGURE 4. Tracking errors in Set 1 of Case I.

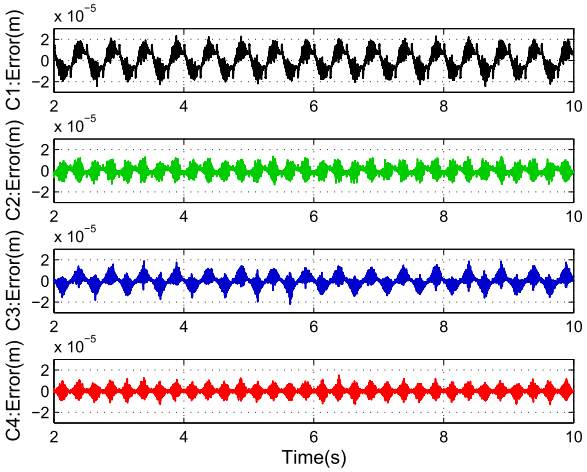

FIGURE 5. Tracking errors in Set 2 of Case I.

performance, thus Case I just shows the the steady-state tracking performance while the related transient performance discrepancy is similar to that in Case II and III. Seen from Table 1, the four tested controllers all achieve good steady-state tracking accuracy during fast sinusoidal motion. Specifical speaking, in Set1, the tracking errors showed in Fig. 4 illustate that e_{RMS} of C4 is about $2.5\mu m$, while C2 and C3 both achieve around $3.4\mu m$, and C1 achieves $6.5\mu m$. It can be seen that, C2 and C3 outperforms C1 on tracking performance, while C4 outperforms C2 and C3 a lot. In Set2, the tracking errors showed in Fig. 5 also illustrate that C4 is the best —e_{RMS} of C4 is 2.38 μm, while e_{RMS} of C2 is $3.21\mu m$

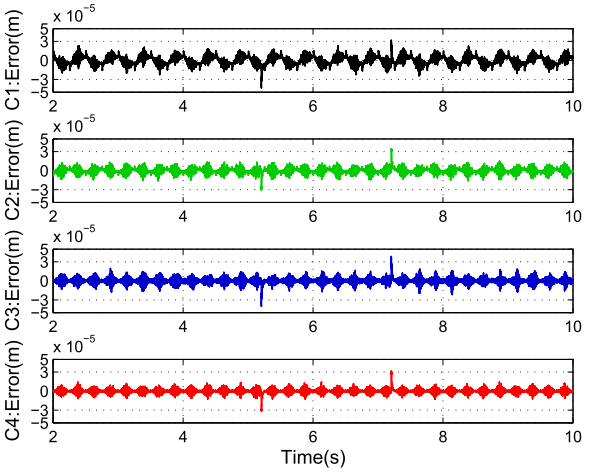

FIGURE 6. Tracking errors in Set 3 of Case I.

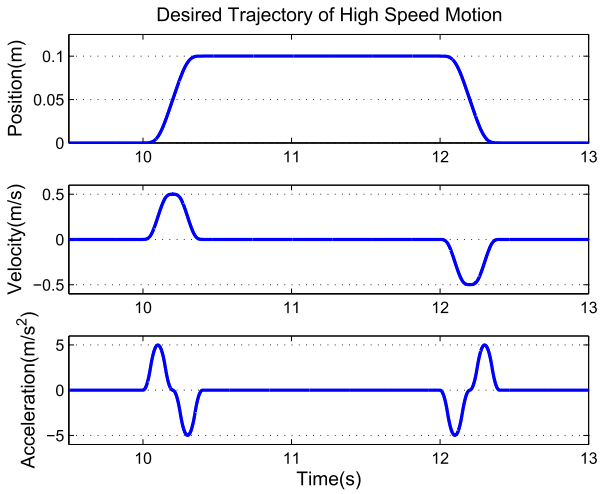

FIGURE 7. Desired trajectory of a high-speed point-to-point motion.

as C2 and C4 both have robustness to parameter variations. In this set, the performance of C3 deteriorate obviously: the e_{RMS} becomes $4.16\mu m$, i.e., 21% enlargement; the e_M becomes $20.8\mu m$, i.e., 26% enlargement, which means that the ILC control input is just the optimum for no-load case but not for 12kg payload case. It also can be concluded that C4 possesses parameter variation robustness. In Set3, the fixed load in Set2 is removed, and an unexpected disturbance is added into the control input. Figure 6 shows the steady tracking errors and the result here further verify that C4 obtains the best accuracy. By comparison among the error signals, it is obvious that C4 possesses performance robustness of C2 to unknown disturbance. To summarize, the above comparative results verify that the proposed LARC control strategy can achieve excellent tracking performance with uncertain disturbance robustness.

2) CASE II—HIGH-SPEED POINT-TO-POINT MOTION TRACKING

As shown in Fig. 7, a point-to-point trajectory is tested with a maximum speed of $v_{max} = 0.5m/s$ and a maximum acceleration of $a_{max} = 5m/s^2$. Set1 and Set2 are implemented in this case.

TABLE 2. Tracking performance indexes in Case II.

Controller		C1: PID	C2: ARC	C3: ILC	C4: LARC
Set1	$e_{RMS}(\mu m)$	4.37	2.78	1.52	1.19
	$e_M(\mu m)$	15.0	8.71	6.47	6.13
Set2	$e_{RMS}(\mu m)$	6.50	3.06	2.84	1.30
	$e_M(\mu m)$	17.2	9.82	9.13	5.60

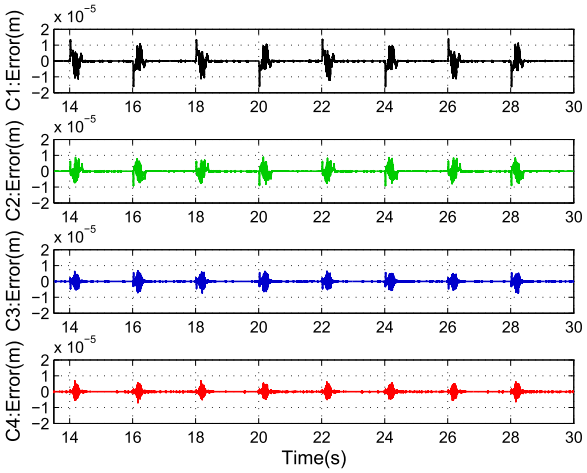

FIGURE 8. Tracking errors in Set1 of Case II.

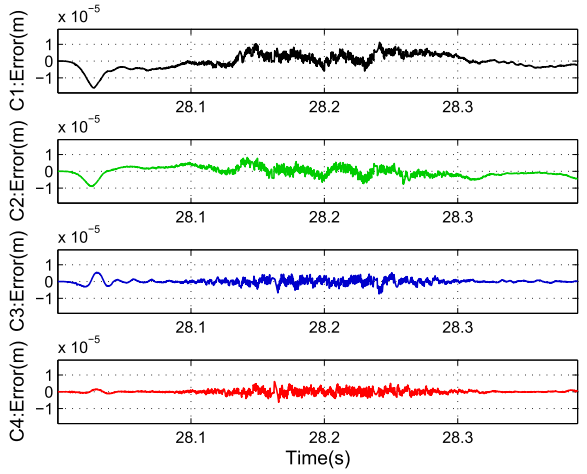

FIGURE 9. Magnified error plots over running period in Set1 of Case II.

Table 2 shows the experimental results after running the linear motor for several periods. e_{RMS} and e_M in the table are the RMS and Maximum of tracking error just at the point-to-point motion segments while the positioning error in the steady-positioning segments are not used. Fig. 8 shows the tracking errors of C1-C4 in Set1, and Fig. 9 shows the magnified error over the running period. It can be seen from the table and the figures that, C4 is rather better than other three controllers — $e_{RMS} = 1.19\mu m$ of C4 is much smaller than the others. In Set2, the 12kg payload is fixed on the motor mover to test the parameter variations robustness of

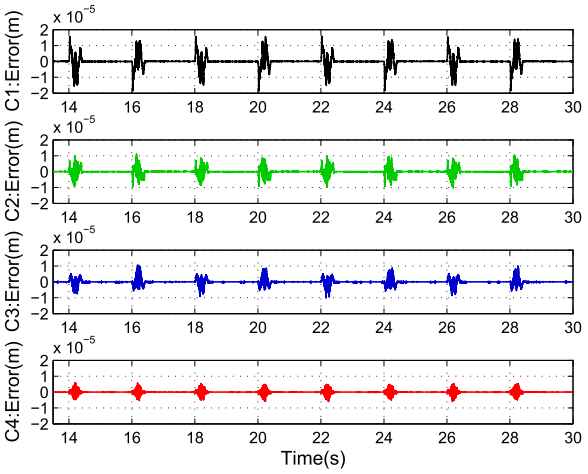

FIGURE 10. Tracking errors in Set2 of Case II.

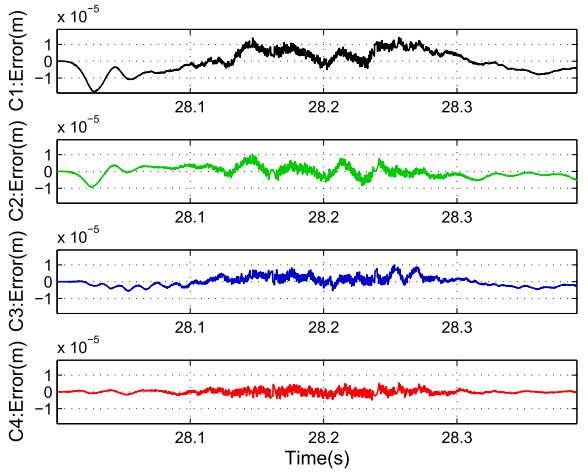

FIGURE 11. Magnified error plots over running period in Set2 of Case II.

the algorithms. Fig. 10 shows the tracking errors of all controllers, and Fig. 11 shows the magnified error over the running period. It can be seen from these plots that, the tracking accuracy of C1 and C3 deteriorates obviously when the payload is added. For example, e_{RMS} of C3 becomes $2.84\mu m$, i.e., 87% enlargement, while e_M of C3 becomes $9.13\mu m$, i.e., 41% enlargement. On the other hand, C2 and C4 perform as well as in the no-load situation of Set1. These results illustrate that online parameter adaptation is important when true parameter values differ from their nominal values. And it also shows that the proposed LARC possesses performance robustness.

It should be pointed out that, in Case II ILC seems to outperform ARC, while in Case I ILC performs at the same level as ARC. The reason is that in the sinusoidal tracking motion, the adjustable model compensation term in ARC contribute to the performance improvement. However, in Case II, i.e., the point-to-point motion, the tracking period is very short while the positioning period is comparatively long, which leads to the function reduction of the model compensation term, especially the friction compensation.

TABLE 3. Tracking performance indexes in Case III.

Controller		C1:PID	C2:ARC	C3:ILC	C4:LARC
$V_M =$ $0.02m/s$	$e_{RMS}(\mu m)$	1.08	0.82	0.26	0.22
	$e_M(\mu m)$	15.86	11.85	3.94	3.25
$V_M =$ $0.002m/s$	$e_{RMS}(\mu m)$	0.96	0.65	0.37	0.18
	$e_M(\mu m)$	9.54	6.37	4.29	1.98
$V_M =$ $0.0002m/s$	$e_{RMS}(\mu m)$	0.33	0.29	0.22	0.19
	$e_M(\mu m)$	2.20	1.96	0.66	0.58

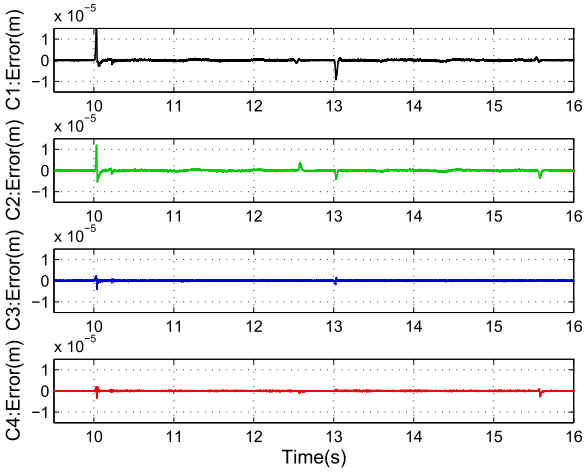

FIGURE 12. Tracking errors of Case3 (V_M=0.02 m/s).

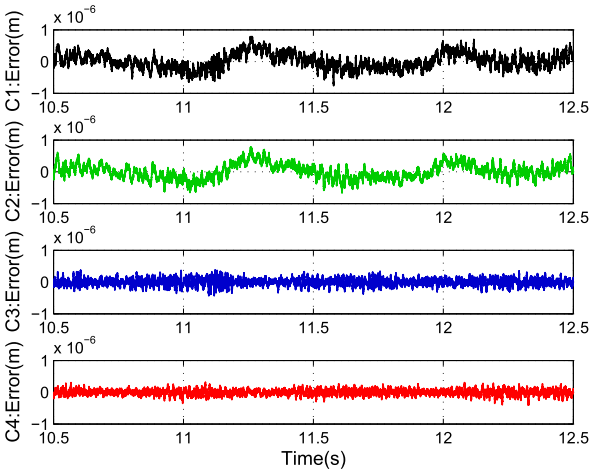

FIGURE 13. Magnified error plots over constant speed period of Case3 (V_M=0.02 m/s).

3) CASE III—LOW-SPEED POINT-TO-POINT MOTION TRACKING

The maximum constant maximum speed v_{max} is set as $0.02m/s$, $0.002m/s$, $0.0002m/s$, the maximum acceleration a_{max} is $0.5m/s^2$, $0.05m/s^2$, $0.005m/s^2$, while the motion distance is $0.05m$, $0.005m$, $0.0005m$, respectively. For these slow motion experiments, the resolution of the grating scale is reset to 39.0625nm for position measurement.

The experimental results of $v_{max} = 0.02m/s$, $0.002m/s$, $0.0002m/s$, are listed in Table 3, respectively. Similar to Case II, e_{RMS} and e_M here are the RMS and Maximum values

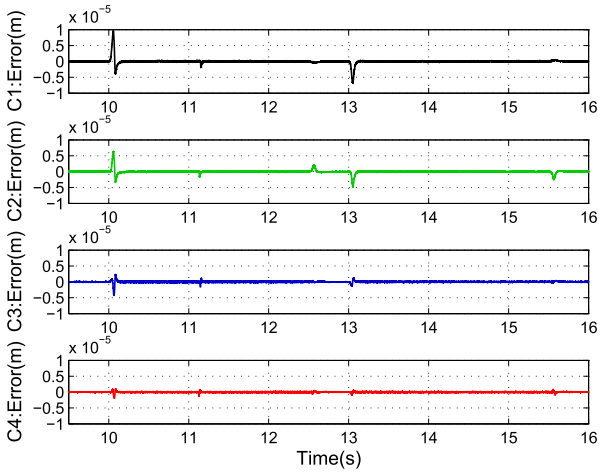

FIGURE 14. Tracking errors of Case3 (V_M=0.002 m/s).

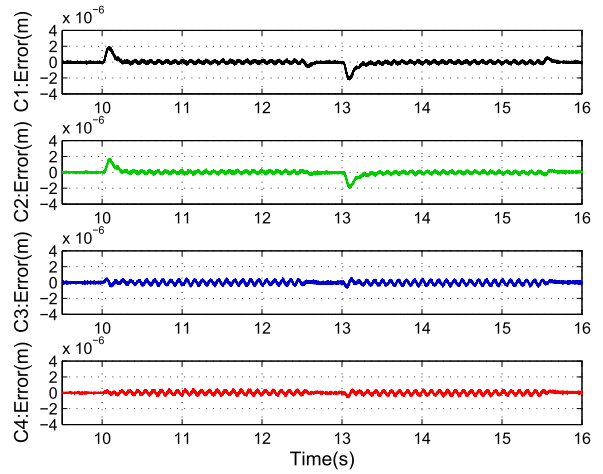

FIGURE 15. Tracking errors of Case3 (V_M=0.0002 m/s).

of tracking error in the point-to-point motion segments while the positioning error in the steady-positioning segments are not used. In Fig. 12, the tracking errors of four controllers are showed for $v_{max} = 0.02m/s$ with the blowout portions for the constant-speed motion plotted in Fig. 13. In Fig. 14, the tracking errors of four controllers are plotted for $v_{max} = 0.002m/s$, and in Fig. 15, the tracking errors of four controllers are showed for $v_{max} = 0.0002m/s$. It can be observed from the table and figures that the proposed LARC algorithm achieves excellent performances in all three low speeds. The tracking errors of LARC in acceleration and deceleration periods are all within $3.25\mu m$, and the errors in constant speed motion period are all within a few hundred nanometers. For example, in the $v_{max} = 0.002m/s$ case, the tracking errors of constant-speed portions showed in Fig. 13 are obviously within 400nm. All these results consistently illustrate that the proposed LARC scheme performs well in low-speed motions as well.

4) CASE IV—ADDITIONAL COMPARATIVE EXPERIMENTS

To further evaluate the practical superiority of the proposed LARC method, the zero phase error tracking

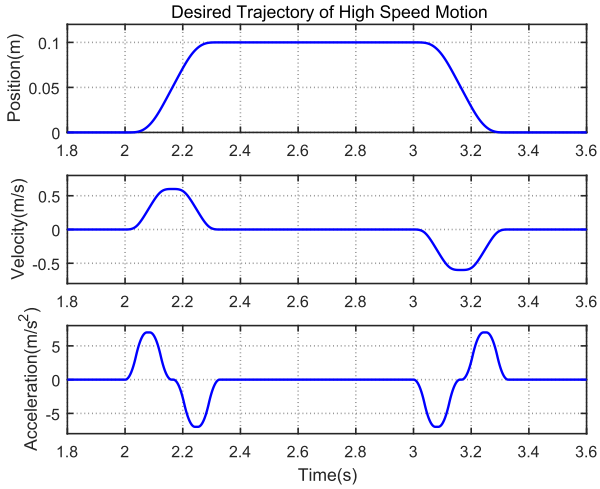

FIGURE 16. Desired high-speed point-to-point trajectory of Case V.

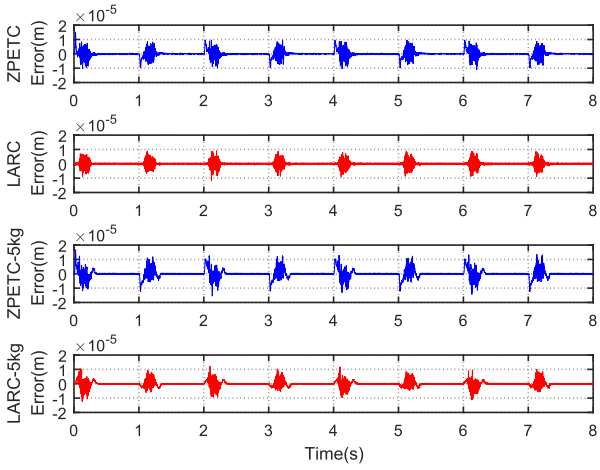

FIGURE 17. Tracking errors of Case V.

TABLE 4. Tracking performance indexes in Case V.

Controller		ZPETC	LARC
No payload	$e_{RMS}(\mu m)$	1.81	1.09
	$e_M(\mu m)$	15.1	11.6
$5kg$ payload	$e_{RMS}(\mu m)$	2.56	1.48
	$e_M(\mu m)$	16.7	12.3

controller (ZPETC) is implemented for comparison. ZPETC is an well-known efficacious feedforward method to improve tracking accuracy, which achieves zero phase error and unity DC gain frequency response [37]. A ZPETC feedforward term is synthesized based on the PID closed-loop response obtained in Case IV, where stable poles and well-damped zeros are kept while unstable and lightly damped zeros are compensated. A high-speed point-to-point trajectory with a maximum speed $v_{max} = 0.6m/s$ and maximum acceleration $a_{max} = 7m/s^2$ plotted in Fig. 16 is carried out in this case. Besides, a $5kg$ payload is added to justify the robustness. Experimental results are illustrated in Fig. 17 and Table 4.

From Fig. 16-17 and Table 4, for no payload and 5kg payload situation, the e_{RMS} of LARC decrease 48% and 42% comparing to ZPETC, while the e_M of LARC decrease 23% and 26%, respectively. These similar improvements of performance indexes indicate that LARC holds stable performance under different situations. Besides, the tracking accuracy of LARC is significantly better than ZPETC. All these experimental results consistently validate the superior nature of LARC.

IV. CONCLUSION

In this paper, a model-data driven learning adaptive robust control (LARC) strategy has been developed and investigated for mechatronic systems to practically achieve excellent transient/steady tracking performance, and robustness to parametric uncertainty and unknown disturbance. The proposed LARC scheme includes adaptive compensation term, robust control term, and iterative learning term, for the modeled dynamics, uncertain nonlinearities, and unmodelled repetitive dynamics, respectively. Comparative experiments have been implemented on a linear motor for a case study. Sufficient results consistently verify that the proposed LARC scheme performs with excellent tracking accuracy even under parametric variations and disturbances. The proposed LARC controller design for linear motor stage systems essentially provides a practically effective motion control technology for industrial applications, and also supplies another perspective which could be followed with extensive researches in the future.

REFERENCES

[1] Y. Jiang, Y. Zhu, K. Yang, C. Hu, and D. Yu, "A data-driven iterative decoupling feedforward control strategy with application to an ultraprecision motion stage," *IEEE Trans. Ind. Electron.*, vol. 62, no. 1, pp. 620–627, Jan. 2015.

[2] C. Hu, Z. Wang, Y. Zhu, M. Zhang, and H. Liu, "Performance-oriented precision LARC tracking motion control of a magnetically levitated planar motor with comparative experiments," *IEEE Trans. Ind. Electron.*, vol. 63, no. 9, pp. 5763–5773, Sep. 2016.

[3] G. H. Nguyen, J.-H. Shin, and W.-H. Kim, "Autotuning controller for motion control system based on intelligent neural network and relay feedback approach," *IEEE/ASME Trans. Mechatronics*, vol. 20, no. 3, pp. 1138–1148, Jun. 2015.

[4] H. Zhu, C. K. Pang, and T. J. Teo, "Integrated servo-mechanical design of a fine stage for a coarse/fine dual-stage positioning system," *IEEE/ASME Trans. Mechatronics*, vol. 21, no. 1, pp. 329–338, Feb. 2016.

[5] H. Tang and Y. Li, "A new flexure-based $Y\theta$ nanomanipulator with nanometer-scale resolution and millimeter-scale workspace," *IEEE/ASME Trans. Mechatronics*, vol. 20, no. 3, pp. 1320–1330, Jun. 2015.

[6] M. Sato and M. Toda, "Robust motion control of an oscillatory-base manipulator in a global coordinate system," *IEEE Trans. Ind. Electron.*, vol. 62, no. 2, pp. 1163–1174, Feb. 2015.

[7] H. Zhu and H. Fujimoto, "Mechanical deformation analysis and high-precision control for ball-screw-driven stages," *IEEE/ASME Trans. Mechatronics*, vol. 20, no. 2, pp. 956–966, Apr. 2015.

[8] J. Yang, Y. Zhu, W. Yin, K. Yang, and H. Mu, "LFT structured uncertainty modeling and robust loop-shaping controller optimization for an ultra-precision positioning stage," *IEEE Trans. Ind. Electron.*, vol. 61, no. 12, pp. 7013–7025, Dec. 2014.

[9] M. Li, Y. Zhu, K. Yang, and C. Hu, "A data-driven variable-gain control strategy for an ultra-precision wafer stage with accelerated iterative parameter tuning," *IEEE Trans. Ind. Informat.*, vol. 11, no. 5, pp. 1179–1189, Oct. 2015.

[10] M. Li, Y. Zhu, K. Yang, C. Hu, and H. Mu, "An integrated model-data-based zero-phase error tracking feedforward control strategy with application to an ultraprecision wafer stage," *IEEE Trans. Ind. Electron.*, vol. 64, no. 5, pp. 4139–4149, May 2017, doi: 10.1109/TIE.2016.2562606.

[11] B. Yao and M. Tomizuka, "Adaptive robust control of SISO nonlinear systems in a semi-strict feedback form," *Automatica*, vol. 33, no. 5, pp. 893–900, May 1997.

[12] L. Xu and B. Yao, "Adaptive robust precision motion control of linear motors with negligible electrical dynamics: Theory and experiments," *IEEE/ASME Trans. Mechatronics*, vol. 6, no. 4, pp. 444–452, Dec. 2001.

[13] B. Yao, C. X. Hu, L. Lu, and Q. F. Wang, "Adaptive robust precision motion control of a high-speed industrial gantry with cogging force compensations," *IEEE Trans. Control Syst. Technol.*, vol. 19, no. 5, pp. 1149–1159, Sep. 2011.

[14] C. Hu, B. Yao, and Q. Wang, "Integrated direct/indirect adaptive robust contouring control of a biaxial gantry with accurate parameter estimations," *Automatica*, vol. 26, no. 4, pp. 701–707, 2010.

[15] C. Hu, Z. Hu, Y. Zhu, and Z. Wang, "Advanced GTCF-LARC contouring motion controller design for an industrial X–Y linear motor stage with experimental investigation," *IEEE Trans. Ind. Electron.*, vol. 64, no. 4, pp. 3308–3318, Apr. 2017.

[16] X. Zhu, G. Tao, B. Yao, and J. Cao, "Adaptive robust posture control of a parallel manipulator driven by pneumatic muscles," *Automatica*, vol. 44, no. 9, pp. 2248–2257, 2008.

[17] A. Mohanty and B. Yao, "Integrated direct/indirect adaptive robust control of hydraulic manipulators with valve deadband," *IEEE/ASME Trans. Mechatronics*, vol. 16, no. 4, pp. 707–715, Aug. 2011.

[18] Z. Chen, B. Yao, and Q. Wang, "μ-synthesis-based adaptive robust control of linear motor driven stages with high-frequency dynamics: A case study," *IEEE/ASME Trans. Mechatronics*, vol. 20, no. 3, pp. 1482–1490, Jun. 2015.

[19] Z. Chen, B. Yao, and Q. Wang, "Accurate motion control of linear motors with adaptive robust compensation of nonlinear electromagnetic field effect," *IEEE/ASME Trans. Mechatronics*, vol. 18, no. 3, pp. 1122–1129, Jun. 2013.

[20] S. Arimoto, S. Kawamura, and F. Miyazaki, "Bettering operation of robots by learning," *J. Robot. Syst.*, vol. 1, no. 2, pp. 123–140, 1984.

[21] B. Altin and K. Barton, "Robust iterative learning for high precision motion control through $\mathcal{L}_1$ adaptive feedback," *Mechatronics*, vol. 24, no. 6, pp. 549–561, 2014.

[22] S. Mishra and M. Tomizuka, "Projection-based iterative learning control for wafer scanner systems," *IEEE/ASME Trans. Mechatronics*, vol. 14, no. 3, pp. 388–393, Jun. 2009.

[23] D. Yu, Y. Zhu, K. Yang, C. Hu, and M. Li, "A time-varying Q-filter design for iterative learning control with application to an ultra-precision dual-stage actuated wafer stage," *Proc. Inst. Mech. Eng., I, J. Syst. Control Eng.*, vol. 228, no. 9, pp. 658–667, 2014.

[24] W. Chen and M. Tomizuka, "Dual-stage iterative learning control for MIMO mismatched system with application to robots with joint elasticity," *IEEE Trans. Control Syst. Technol.*, vol. 22, no. 4, pp. 1350–1361, Jul. 2014.

[25] H.-S. Ahn, Y. Q. Chen, and K. L. Moore, "Iterative learning control: Brief survey and categorization," *IEEE Trans. Syst., Man, Cybern. C, Appl. Rev.*, vol. 37, no. 6, pp. 1099–1121, Nov. 2007.

[26] D. A. Bristow, M. Tharayil, and A. G. Alleyne, "A survey of iterative learning control," *IEEE Control Syst. Mag.*, vol. 26, no. 3, pp. 96–114, Jun. 2006.

[27] I. Rotariu, M. Steinbuch, and R. Ellenbroek, "Adaptive iterative learning control for high precision motion systems," *IEEE Trans. Control Syst. Technol.*, vol. 16, no. 5, pp. 1075–1082, Sep. 2008.

[28] W. Liu, L. Cheng, Z.-G. Hou, J. Yu, and M. Tan, "An inversion-free predictive controller for piezoelectric actuators based on a dynamic linearized neural network model," *IEEE/ASME Trans. Mechatronics*, vol. 21, no. 1, pp. 214–226, Feb. 2016.

[29] L. Xu and B. Yao, "Adaptive robust repetitive control of a class of nonlinear systems in normal form with applications to motion control of linear motors," in *Proc. IEEE/ASME Conf. Adv. Intell. Mechatronics (AIM)*, Como, Italy, Jul. 2001, pp. 527–532.

[30] J. Q. Gong and B. Yao, "Neural network adaptive robust control of SISO nonlinear systems in a normal form," *Asian J. Control*, vol. 3, no. 2, pp. 96–110, 2001.

[31] C. Hu, B. Yao, Z. Chen, and Q. Wang, "Adaptive robust repetitive control of an industrial biaxial precision gantry for contouring tasks," *IEEE Trans. Control Syst. Technol.*, vol. 19, no. 6, pp. 1559–1589, Nov. 2011.

[32] M. French and E. Rogers, "Non-linear iterative learning by an adaptive Lyapunov technique," *Int. J. Control*, vol. 73, no. 10, pp. 840–850, 2000.
[33] Z. Hu, C. Hu, Y. Zhu, and J. Yang, "Performance-oriented investigation of adaptive robust control in iterative learning control framework with comparative experiments," in *Proc. IEEE Int. Conf. Adv. Intell. Mechatronics*, Jul. 2015, pp. 743–748.
[34] Z. Wang, C. Hu, Y. Zhu, and M. Zhang, "Precision LARC motion controller design for a magnetically levitated planar motor," in *Proc. IEEE Int. Conf. Inf. Automat.*, Aug. 2015, pp. 1359–1364.
[35] C. Hu, B. Yao, and Q. Wang, "Global task coordinate frame-based contouring control of linear-motor-driven biaxial systems with accurate parameter estimations," *IEEE Trans. Ind. Electron.*, vol. 58, no. 11, pp. 5195–5205, Nov. 2011.
[36] C. Hu, B. Yao, Q. Wang, Z. Chen, and C. Li, "Experimental investigation on high-performance coordinated motion control of high-speed biaxial systems for contouring tasks," *Int. J. Mach. Tools Manuf.*, vol. 51, no. 9, pp. 677–686, Sep. 2011.
[37] M. Tomizuka, "Zero phase error tracking algorithm for digital control," *ASME Trans. J. Dyn. Syst. Meas. Control*, vol. 109, no. 1, pp. 65–68, Mar. 1987.

CHUXIONG HU (S'09–M'11–SM'16) received the B.S. and Ph.D. degrees in mechatronic control engineering from Zhejiang University, Hangzhou, China, in 2005 and 2010, respectively.

From 2007 to 2008, he was a Visiting Scholar with the Mechanical Engineering Department, Purdue University, West Lafayette, USA. In 2018, he was a Visiting Scholar with the Mechanical Engineering Department, University of California, Berkeley, USA. He is currently an Associate Professor with the State Key Laboratory of Tribology, Department of Mechanical Engineering, Tsinghua University, Beijing, China. His research interests include intelligent control, precision motion control, high-performance multi-axis contouring control, precision mechatronic systems, adaptive robust control, iterative learning control, neural networks, and precision metrology/measurement calibration.

Dr. Hu was a recipient of the 2013 National 100 Excellent Doctoral Dissertations Nomination Award of China and the 2016 Best Automation Paper Award. He received the Best Student Paper Finalist at the 2011 American Control Conference, the 2012 Best Mechatronics Paper Award from the ASME Dynamic Systems and Control Division, and the 2018 Best AI Paper Award from the IEEE Internal Conference on Information and Automation.

ZHIPENG HU received the B.S. degree in mechanical engineering from Tsinghua University, Beijing, China, in 2015, and the master's degree from the Mechanical Engineering Department, Stanford University, Beijing, in 2017. He is currently with Tesla Cop., CA, USA. His research interests include precision motion control and robotic manipulation.

YU ZHU (M'12) received the B.S. degree in radio electronics from Beijing Normal University, Beijing, China, in 1983, and the M.S. degree in computer applications and the Ph.D. degree in mechanical design and theory from the China University of Mining and Technology, Beijing, in 1993 and 2001, respectively.

He is currently a Professor with the State Key Laboratory of Tribology, Department of Mechanical Engineering, Tsinghua University, Beijing. He has published more than 200 technical papers. He holds more than 150 warranted invention patents. His research interests include precision measurement and motion control, precision mechanical design and manufacturing, two-photon micro-fabrication, and electronics manufacturing technology and equipment.

ZE WANG received the B.S. degree in automation from the School of Electricity Engineering and Automation, Tianjin University, Tianjin, China, in 2015. He is currently pursuing the Ph.D. degree in mechanical engineering with the Department of Mechanical Engineering, Tsinghua University, Beijing, China. His research interests include precision motion control, NN control, adaptive control, and high-performance multi-axis contouring control.

SUQIN HE received the B.S. degree in mechanical engineering from the Department of Mechanical Engineering, Tsinghua University, Beijing, China, in 2016, where he is currently pursuing the Ph.D. degree in mechanical engineering. His research interests include precision motion control and robot manipulator control.